A Journal of the Gesellschaft Deutscher Chemiker

Angewandte International Edition GDCh Chemie

www.angewandte.org

Accepted Article

Title: Ambient Electro-Synthesis of Ammonia-Electrode Porosity and Composition Engineering

Authors: Geoffrey A. Ozin, Hong Wang, Lu Wang, Qiang Wang, Shuyang Ye, Wei Sun, Yue Shao, Zhiping Jiang, Qiao Qiao, Yimei Zhu, Pengfei Song, Debao Li, Le He, Xiaohong Zhang, Jiayin Yuan, and Tom Wu

This manuscript has been accepted after peer review and appears as an Accepted Article online prior to editing, proofing, and formal publication of the final Version of Record (VoR). This work is currently citable by using the Digital Object Identifier (DOI) given below. The VoR will be published online in Early View as soon as possible and may be different to this Accepted Article as a result of editing. Readers should obtain the VoR from the journal website shown below when it is published to ensure accuracy of information. The authors are responsible for the content of this Accepted Article.

To be cited as: *Angew. Chem. Int. Ed.* 10.1002/anie.201805514
Angew. Chem. 10.1002/ange.201805514

Link to VoR: http://dx.doi.org/10.1002/anie.201805514
http://dx.doi.org/10.1002/ange.201805514

WILEY-VCH

10.1002/anie.201805514

WILEY-VCH

Ambient Electro-Synthesis of Ammonia - Electrode Porosity and Composition Engineering

Hong Wang‡*, Lu Wang‡, Qiang Wang, Shuyang Ye, Wei Sun, Yue Shao, Zhiping Jiang, Qiao Qiao, Yimei Zhu, Pengfei Song, Debao Li, Le He, Xiaohong Zhang, Jiayin Yuan*, Tom Wu, Geoffrey A. Ozin*

Abstract: Ammonia, key precursor for fertilizer production, convenient hydrogen carrier and emerging clean fuel, plays a pivotal role in sustaining life on earth. Currently, the main route for NH_3 synthesis is via the heterogeneous catalytic Haber-Bosch process ($N_2+3H_2 \rightarrow 2NH_3$), which proceeds under extreme conditions of temperature and pressure with a very large carbon footprint. Herein we report that a pristine nitrogen-doped nanoporous graphitic carbon membrane (NCM) can electrochemically convert N_2 into NH_3 in an aqueous acidic solution under ambient conditions. The Faradaic efficiency and rate of production of NH_3 on the NCM electrode reach 5.2% and 0.08 g m^{-2} h^{-1}, respectively. After functionalization of the NCM with Au nanoparticles (Au NPs) these performance metrics are dramatically enhanced to 22% and 0.36 g m^{-2} h^{-1}, respectively. As this system offers the potential to be scaled to industrial proportions there is a high likelihood it might displace the century old Haber-Bosch process.

Fixation of N_2 to NH_3 is an essential process for maintaining life on earth[1-4]. Currently, NH_3 production is dominated by the Haber–Bosch process. It operates under conditions of high temperature 400–500 °C and pressure 200–250 bar, and its production has a huge carbon footprint[5]. The H_2 precursor, usually obtained by steam reforming of methane, also has a very large carbon footprint. Notably, the entire energy required to prepare the reagents and to operate the Haber-Bosch process amounts to 1–3% of the global energy supply[6]. In stark contrast, in the natural world, plants and bacteria have been producing NH_3 from N_2 and solvated protons under ambient conditions, enabled by the FeMo cofactor of the metalloenzyme nitrogenase ($N_2 + 6H^+ 6e^- \rightarrow 2NH_3$)[7, 8]. Inspired by this biological nitrogen fixation process, intensive efforts have been devoted to finding ways to mimic the process under similarly mild conditions.

To this end, the electrocatalytic N_2 reduction reaction (NRR) conducted in an aqueous media has recently been receiving increasing attention. This approach offers multiple merits: (i) use of water as the hydrogen source, (ii) operation under ambient conditions, and (iii) utilization of renewable electricity to drive the process[9-10]. Nonetheless, the extremely high bond energy of the N_2 molecule, 940.95 kJ mol^{-1} together with its lack of a permanent dipole, makes running the NRR under mild conditions extremely challenging[11]. The quest for suitable electrocatalysts and electrolytes for the NRR represents one of the most active areas of materials and energy research[12-17]. Among the electrocatalysts and electrolytes for the NRR, the most efficient ones rely on high temperature reactions (T> 200 °C) to favor the reaction thermodynamics. For example, Licht et al. found that an electrochemical cell constructed with a Ni electrode and a ternary molten hydroxide (KOH/NaOH/CsOH) suspension of nano-Fe_2O_3 could produce NH_3 at a coulombic efficiency of 35% by electrolysis of air and steam at 200 °C[18]. Marnellos et al. demonstrated that a Pd electrode in combination with $ScCe_{0.95}Yb_{0.05}O_{3-\alpha}$ as a solid-state proton conductor could generate NH_3 with a Faradaic efficiency of 78% by electrolysis of N_2 and H_2 at 570 °C[19].

Herein we report for the first time that hierarchically structured nitrogen-doped nanoporous carbon membranes (NCMs) can electrochemically convert N_2 into NH_3 at room temperature and atmospheric pressure in an acidic aqueous solution. The Faradaic efficiency and rate of NH_3 production using the metal-free NCM electrode in 0.1 M HCl solution are as high as 5.2% and 0.08 g m^{-2} h^{-1}, respectively. Upon functionalization of the NCM electrode with Au nanoparticles (Au NPs), the efficiency and rate are boosted to a remarkable 22% and 0.36 g m^{-2} h^{-1}, respectively. These performance metrics are unprecedented for the electrocatalytic production of NH_3 from N_2 under ambient conditions.

To amplify, **Fig. 1a-c** shows the synthetic protocol for making NCMs (see details in Supplementary information). To begin, a homogeneous dispersion of multi-wall CNTs was prepared by sonicating CNTs in a solution of poly(acrylic acid) (PAA) and a poly(ionic liquid) named poly[1-cyanomethyl-3-vinylimidazolium bis(trifluoromethanesulfonyl)imide] (PCMVImTf$_2$N) in N,N-dimethyl formamide (**Fig. 1a**). The chemical structures of PCMVImTf$_2$N and PAA are shown in **Fig. S1**. The stable

[*] Dr. H. Wang, Mr. Y. Shao, Miss. Z. Jiang
Key Laboratory of Functional Polymer Materials of the Ministry of Education, Institute of Polymer Chemistry, College of Chemistry, Nankai University, Tianjin, 300071, P. R. China
E-mail: hongwang1104@nankai.edu.cn
Dr. L. Wang, Mr. S. Ye, Dr. W. Sun, Prof. G. A. Ozin
Materials Chemistry and Nanochemistry Research Group, Solar Fuels Cluster, Centre for Inorganic and Polymeric Nanomaterials, Departments of Chemistry, Chemical Engineering and Applied Chemistry, and Electrical and Computing Engineering, University of Toronto
80 St. George Street, Toronto, Ontario M5S3H6 (Canada)
E-mail: gozin@chem.utoronto.ca
Dr. L. Wang, Prof. L. He, Prof. X. Zhang
Institute of Functional Nano & Soft Materials, Soochow University, Suzhou, Jiangsu 215123, P. R. China
Dr. Q. Wang, Dr. D. Li
State Key Laboratory of Coal Conversion, Institute of Coal Chemistry, The Chinese Academy of Sciences, Taiyuan 030001, China
Dr. Q. Qiao
Department of Physics, Temple University, Philadelphia, Pennsylvania 19122, USA; Condensed Matter Physics and Materials Science Department, Brookhaven National Laboratory, Upton, New York 11973, USA
Dr. Y. Zhu
Condensed Matter Physics and Materials Science Department, Brookhaven National Laboratory, Upton, New York 11973, USA
Prof. P. Song
College of Chemistry and Chemical Engineering, Northwest Normal University, Lanzhou 730070, P.R. China
Prof. J. Yuan
Department of Materials and Environmental Chemistry, Stockholm University, 10691, Stockholm, Sweden
Email: jiayin.yuan@mmk.su.se
Prof. T. Wu
School of Materials Science and Engineering, UNSW Australia, Kensington Campus Building E10, Sydney, NSW 2052, Australia
‡Authors contributing equally to the work.

Accepted Manuscript

This article is protected by copyright. All rights reserved.

polymer/CNT dispersion was cast onto a glass plate, dried at 80 °C into a sticky black film, and finally immersed in an aqueous NH_3 solution (0.1wt %) to build up a nanoporous polymer/CNT hybrid membrane (**Fig. 1b**, **Fig. S2**). Afterwards, pyrolysis treatment of the hybrid membrane at 900 ºC under N_2 leads to the targeted NCM (**Fig. 1c**). The porous surface can be seen from the top view of the NCM in a SEM image (**Fig. 1d**). **Fig. 1e** shows that a three-dimensionally interconnected macroporous architecture was created along the cross-section. A high-magnification SEM image (**Fig. 1f**) reveals that CNTs are uniformly embedded in the NCM, which is expected owing to their uniform dispersion in the PCMVImTf$_2$N/PAA DMF solution.

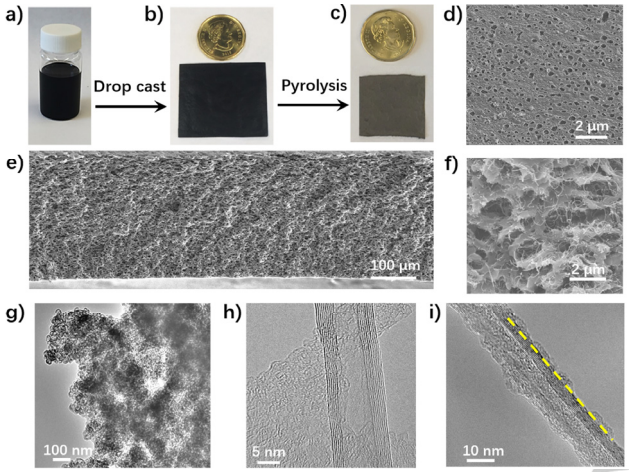

Figure 1. a)-c), Scheme illustrating the synthetic route to the NCM. Image (a) depicts a homogeneous dispersion of CNTs in a solution of PCMVImTf$_2$N and PAA in DMF; Image (b) is a PCMVImTf$_2$N/PAA/CNT hybrid membrane; Image (c) is a NCM prepared from pyrolysis of sample in (b); d), SEM image of the top surface of the NCM. e), f), Low- and high-magnification cross-section SEM images of the NCM, respectively. g, a HRTEM image of NCM. h), a single native CNT. i), the core-shell structure of a CNT-NC heterojunction. The yellow arrow directed area represents N-doped carbon sheath attached to a CNT.

The microstructure of the NCM was further analyzed by high-resolution transmission electron microscopy (HRTEM), in which CNTs embedded in the nanoporous carbon membrane matrix are clearly identified (**Fig. 1g**, **Fig. S3**). The well-defined lattice spacing of 0.34 nm indicates that the NCM membrane contains highly organized graphitic domains (**Fig. S4**). The individual graphitic layers can be seen to bend due to a doping effect of nitrogen atoms, and extend practically across the entire membrane. The content of nitrogen is 9.0 wt. % as determined by elemental analysis. **Fig. 1h** shows a HRTEM image of a native CNT, which is typically composed of 7-12 layers with an outer diameter of 5-10 nm. Notably, in **Fig. 1i** and **Fig. S5**, a thin rough sheath is formed on the CNT wall (see the area indicated by the yellow arrow), referred to as a CNT-NC core-shell microstructure. We previously demonstrated that the imidazolium cations, a major component in PCMVImTf$_2$N polymer, could attach to the graphitic CNT surface owing to the well-known cation-π interaction for dispersion purposes[20]. It has recently been reported that the CNT surface could template and catalyze the pyrolysis of ionic liquid species to form structural motifs different from their bulk carbonization[21]. The newly formed sheath of N-doped carbon on the surface of CNT is rich in defects (dangling bonds) and short-range ordered micropores. Specifically, the heteroatoms, through templating interactions, favorably align themselves at the CNT surface for exposure to reagents, thereby enabling high electron transfer efficiency via charge transfer interactions, which in turn will modify catalytic activity.

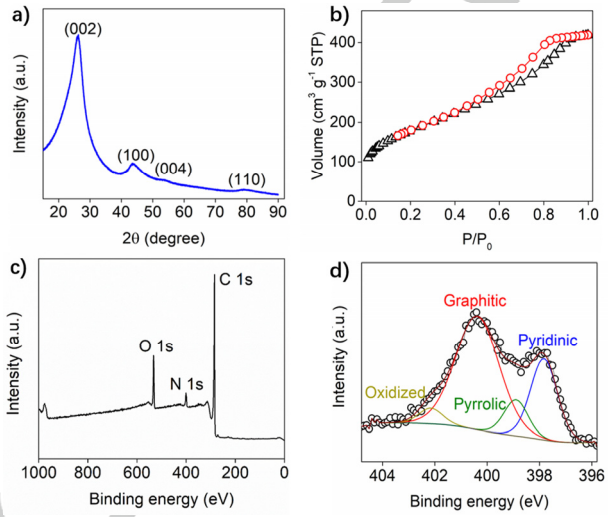

Figure 2. a), XRD pattern of the NCM. b), BET specific surface area of the NCM. c), XPS spectrum of the NCM. d), High-resolution N1 XPS spectrum of the NCM and its deconvolution into four chemically distinct N forms.

Fig. 2a shows the X-ray diffraction (XRD) pattern of the NCM. Sharp diffraction peaks at 26°, 44°, 53° and 80° are observed and attributed to the (002), (100), (004) and (112) reflections of a graphitic carbon, respectively. Such a graphitic structure of the NCM endows it with high electronic conductivity (134 S cm^{-1} at 298 K)[22], which favors fast charge transport, a mandatory requirement for efficient electrocatalysis.

Specific surface area plays an essential role in optimizing catalytic activity of heterogeneous catalysts. The Brunauer-Emmett-Teller (BET) specific surface area of NCM (**Fig. 2b**) is measured to be 432 m^2/g with a pore volume of 0.58 cm^3/g. It is clear from the imaging and pore size distribution (**Fig. S6**) studies that the pore architecture of the NCM membrane is hierarchical in nature, comprising of macropores seen in the cross-sectional image with pores traversing the entire micro- to meso- to macropore range. In such hierarchically porous membrane architectures, micropores and small mesopores are beneficial to provide large and accessible surface area. Plus the large mesopores and macropores form interconnected three-dimensional networks, which can serve as transport highways to accelerate mass diffusion and promote electron exchange efficiency and catalytic activity. Furthermore, the hierarchical porous architecture and favorable electrical conductivity of the NCM allow it to function as a diffusion electrode to enhance the three-phase contact and charge transport between the heterogeneous electrocatalyst, aqueous electrolyte and gaseous reactants to optimize the electrocatalytic reaction rate.

X-ray photoelectron spectroscopy (XPS) show diagnostic C, N and O peaks in the NCM (**Fig. 2c**), and provide evidence that the NCM is metal-free. An analysis of different N species in the NCM structure is presented in **Fig. 2d**. The N 1s XPS spectrum shows that N in the carbon framework exists mainly in the

Accepted Manuscript

This article is protected by copyright. All rights reserved.

pyridinic (398.0 eV), pyrrolic (398.6 eV), graphitic (400.2 eV) and oxidized (402.2 eV) forms with corresponding abundances of 32.2%, 12.9%, 48.1%, 6.8%, respectively. It is relevant that the high pyridinic and pyrrolic N content in NCM, which we attribute to surface templating of the condensation reactions, co-exists with coupled edge termination of graphitic layers by pyridinic-pyrrolic units. It is considered that pyridinic and pyrrolic N atoms are the catalytic active sites in N-doped carbons[23]. Previous reports have demonstrated that dangling bonds are key to NRR activity[13]. Considering that abundant pyridinic and pyrrolic N atoms, considered as dangling bonds, exist in the NCM, in what follows, we will discuss the NRR performance of the NCM in an acidic solution under ambient conditions.

The NCM was directly utilized as the working electrode for the NRR in 0.1 M HCl (pH =1) electrolyte at ambient conditions. Noticeably, a polymer binder, which is mandatory for use of powdered electrocatalysts is not needed to construct the working electrode due to the structural connectivity of the NCM. The N_2 is supplied in a feed gas stream to the diffusion-type porous NCM cathode, where protons (H^+) are transported through the electrolyte to react with N_2 to produce NH_3 (N_2 + 6H+ $6e^- \rightarrow 2NH_3$). We firstly investigated the overpotential required to achieve the maximum Faradaic efficiency of NH_3 synthesis for the NCM electrode from 0 V to -0.4 V (vs RHE). The system was tested for an extended period of 3 hours (**Fig. S7**). The yield of NH_3 produced by the NRR on the NCM electrode was measured by using the indophenol blue method[3,24] (**Fig. S8-9**). The achievable maximum Faradaic efficiency of 5.2% for NH_3 was reached at -0.2 V (vs RHE) (**Fig. 3a**) and the highest rate of NH_3 is 0.08 g m^{-2} h^{-1} at -0.3 V (vs RHE) (**Fig. 4b**, **Fig. S10**). As shown in **Fig. 3b**, the rate of NH_3 decreases significantly beyond -0.3 V (vs RHE), which is attributed to a competitive reduction of N_2 and hydrogen species on the electrode surface. In the case of the Haber-Bosch NH_3 synthesis, N_2H_4 is the major by-product. Notably, in our NCM based electrochemical process, N_2H_4 was not detected (**Fig. S11**), indicative of a 100% selectivity of the NCM for reduction of N_2 to NH_3.

In control experiments, when N_2 was replaced by argon, while keeping other reaction parameters unchanged, NH_3 could not be identified in the electrolyte (**Fig. S12**). The same was observed when the NCM was replaced by a carbon paper or pristine CNTs (**Fig. S13-14**). These control experiments confirmed that NH_3 was produced exclusively from the NRR reaction catalysed by the NCM electrode. In addition, XPS spectra of the NCM after a 4-day stability test were recorded (**Fig. S15**), which show no difference compared to the pristine NCM. Such robust electrochemical stability is likely attributed to the nitrogen doping effect, which improves the electrochemical stability and resistance against oxidation by modifying the electronic band structure of the graphitic carbons.

Note that the NCM was fabricated by direct pyrolysis of a polyelectrolyte complex membrane. It is well known that polyelectrolytes are capable of binding and immobilizing metal ions, salts and nanoparticles[25]. This knowledge inspired us to functionalize the NCM with metal nanoparticles via doping the polymer membrane with metal species before carbonization. In this context we co-assembled Au nanoparticles (Au NPs) with the NCM to amplify the performance of the NCM for the NRR. The detailed synthetic procedure and structural characterizations, including digital photograph, XRD, SEM, TEM, Au NPs size distribution, HRTEM and elemental mappings of the NCM-metal nanoparticle hybrid (NCM-Au NPs) are provided in the Supplementary information and **Fig. S16-21**.

The loading of Au within the NCM was 6.03 wt % as detected by inductively coupled plasma−atomic emission spectra (ICP−AES). The composite NCM-Au NPs electrode for NRR testing was the same as the pristine NCM (**Fig. S22**). The optimised Faradaic efficiency and rate of NCM-Au NPs in conversion of N_2 to NH_3 was as high as 22% at -0.1 V vs RHE (**Fig. 3c**) and 0.36 g m^{-2} h^{-1} at -0.2 V vs RHE (**Fig. 3d**, **Fig. S23**) respectively. Note that there is no NH_4Cl produced in electrolyte without employing applied potential (**Fig. S24**). These are the highest values ever reported for NH_3 production at ambient conditions. Similar to the NCM electrode, there is no N_2H_4 found using the NCM-Au NPs electrode (**Fig. S25**), certifying the 100% selectivity of NCM-Au NPs in this process. Furthermore, to ensure the NH_3 product of the reactions did not originate from adventitious N residues in our samples, isotopically labelled $^{15}N_2$ authenticated the origin of the products of the NRR. We bubbled 20 mL of 0.1 M HCl electrolyte with N_2 using a large piece of NCM-Au NPs (6.5 x 3 cm^2) as the working electrode, Ag/AgCl as reference electrode and Pt as counter electrode under -0.2 V vs RHE (**Fig. 4a**), after reacting for 28 h, the white and slightly yellow product was collected by freeze-drying of the electrolyte. The ^{1}H-NMR spectrum of produced $^{15}NH_4Cl$ shows the doublet peaks (6.89 ppm, J^1_{NH} = 72.2 Hz) (**Fig. 4b**), consistent with previously reported[2], which clearly demonstrated that NCM-Au can efficiently transfer N_2 into NH_3, being potential to be scaled to industrial proportions there is a high likelihood it might displace the century old Haber-Bosch process.

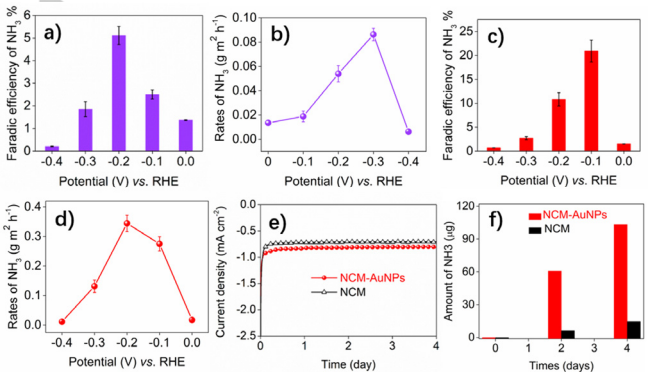

Figure 3. a), Faradaic efficiencies for NH_3 production vs applied potential at the NCM electrode (vs RHE). b), the rates of NH_3 production on the NCM electrode at applied potentials (vs RHE). c), Faradaic efficiencies for NH_3 production vs the applied potential at the NCM-Au NPs electrode (vs RHE). d), the rates of NH_3 production on the NCM-Au NPs electrode at applied potentials (vs RHE). e), Chrono-amperometry results at the corresponding potentials (in a and c) with the highest Faradaic efficiencies. f), the yields of NH_3 production at regular interval times on the NCM and NCM-Au NPs electrodes during a long-term operational stability test.

To gain additional insight into the catalytic kinetics of the NRR, electrochemical impedance spectroscopy measurements were performed at various overpotentials. As shown in **Fig. S26**, Nyquist plots were used to determine the series resistance (R_s), pore resistance (R_p) and charge-transfer resistance (R_{ct}). The

Accepted Manuscript

This article is protected by copyright. All rights reserved.

overpotential-independent behaviour of R_p for NRR (~0.4 Ω/cm^2) indicate the robust nature of the hierarchical pore structure of the catalyst even at high overpotentials, and these structures also serve as efficient channels for mass transport to access the exposed active sites. In addition, NCM-Au NPs exhibited a much lower R_{ct} for NRR (0.047 Ω/cm^2 at 227 mV), indicating fast charge transfer during the reactions due to the highly conductive nature of the NCM-Au NPs.

The stability of an electrocatalyst is key for its practical applications. Both NCM and NCM-Au NPs membranes were operated for 4 days, as shown in **Fig. 3e**. No decay of activity was observed, indicating excellent electrochemical durability for both systems. The yield of NH_3 produced on both NCM and NCM-Au NPs electrodes were measured at regular intervals during the stability test (**Fig. S27-28**), and as shown in **Fig. 3f**, the yield of NH_3 actually was observed to increase with reaction time. This impressive performance clearly demonstrates the robustness of NCM and NCM-Au NPs electrodes for NRR.

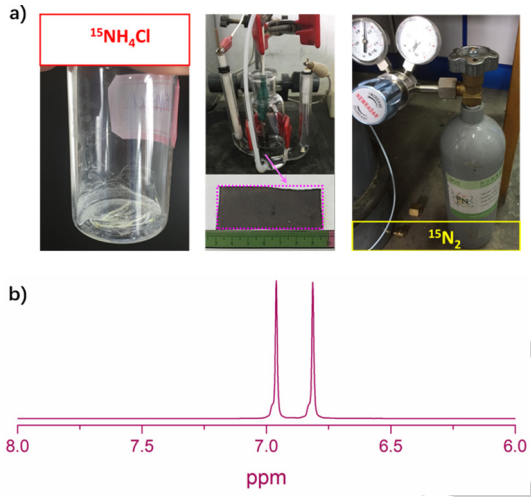

Figure 4. a), Photograph of equipment used for producing $^{15}NH_4Cl$. b), The ^{1}H-NMR spectrum of isolated $^{15}NH_4Cl$ in the above setup.

Although previous theoretical predictions and experimental tests showed that Au nanomaterials are NRR-active, their N_2 reduction yield and product selectivity are limited[26]. In stark contrast, our NCM-Au NPs electrode exhibits unprecedented NRR performance. Firstly, Au NPs homogeneously dispersed and highly embedded within the NCM, could improve carbon–metal interactions and increase the number of chemically active sites[27]. While still under debate, it is generally agreed that the mechanism of the heterogeneously catalysed NRR can be either associative or dissociative[7,28] (**Fig. S29**). For both mechanisms, the first step is N_2 binding to the surface of the heterogeneous catalyst. In our case, the heterojunction between the Au NPs and semiconductor-like NCM, verified by temperature-dependent conductivity measurements, as shown in **Fig. S30**, creates a rectifying e□ect[29]. At the interface of Au/NCM, electrons are expected to flow from NCM to Au (**Fig. S31**), considering the E_f of Au and NCM are -5.0 eV and -4.5 eV, respectively. In this case, the positively charged NCM surface so formed may adsorb N_2 more strongly and thereby improve the NRR activity[28]. Together, the synergistic charge-transfer between Au NPs and NCM creates excellent NRR performance of the NCM-Au NPs electrode (**Table S1**).

Considering the excellent conversion efficiency and selectivity of N_2 to NH_3 by NCM and NCM-AuNP electrodes, and the straightforward method for production of the NCM membranes at scale, the advance described herein provides exciting opportunities for developing a highly efficient, industrial electrochemical process for producing NH_3 from abundant N_2 and H_2O under ambient temperature and pressure conditions. With further optimization of this electrocatalytic system there is an excellent chance it will be able to outcompete the century old heterogeneous catalytic Haber-Bosch process that operates under extreme conditions of temperature and pressure.

Acknowledgements

G.A.O. is a Government of Canada Research Chair in Materials Chemistry and Nanochemistry. Financial support for this work was provided by the Ontario Ministry of Research Innovation (MRI); Ministry of Economic Development, Employment and Infrastructure (MEDI); Ministry of the Environment and Climate Change; Connaught Innovation Fund; Connaught Global Challenge Fund; and the Natural Sciences and Engineering Research Council of Canada (NSERC). J. Y. is grateful for financial support from the ERC Starting Grant NAPOLI - 639720. H. W. acknowledges the financial support from the Nankai University.

Keywords: Poly(ionic liquid) • Porous carbon membrane • Functionalization • Electrocatalysis • Nitrogen fixation •

[1] R. Lan, J. T. S. Irvine, S. Tao, *Sci. Rep*. **2013**, *3*, 1145.
[2] C. Liu, K. K. Sakimoto, B. C. Colón, P. A. Silver, D. G. Nocera, *Proc. Natl. Acad. Sci.* **2017**, *114*, 6450–6455.
[3] D. Zhu, L. Zhang, R. E. Ruther, Hamers, R. J. *Nat. Mater*. **2013**, *12*, 837–841.
[4] J. H. Montoya, C. Tsai, A. Vojvodic, J. K. Norskov, *ChemSusChem*. **2015**, *8*, 2180–2186.
[5] D. Tilman, K. G. Cassman, P. A. Matson, R. Naylor, S. Polasky, *Nature* **2002,** *418*, 671–677.
[6] M. A. H. J. V. Kessel, D. R. Speth, M. Albertsen, P. H. Nielsen, H. J. M. Op den Camp, B. Kartal, M. S. M. Jetten, S. Lücker, *Nature*, **2015**, *528*, 555-559.
[7] C. J. M. Van der Ham, M. T. M. Koper, D. G. H. Hetterscheid, *Chem. Soc. Rev*. **2014**, *43*, 5183–5191.
[8] K. A. Brown, D. F. Harris, M. B. Wilker, A. Rasmussen, N. Khadka, H. Hamby, S. Keable, G. Dukovic, J. W. Peters, L. C. Seefeldt, P. W. King, *Science* **2016**, *352*, 448-450.
[9] S. Gao, Y. Lin, X. Jiao, Y. Sun, Q. Luo, W. Zhang, D. Li, J. Yang, Y. Xie, *Nature*, **2016**, *529*, 68-71.
[10] C. Costentin, M. Robert, J.-M. Saveant, *Chem. Soc. Rev*. **2013**, *42*, 2423–2436.
[11] K. Honkala, A. Hellman, I. N. Remediakis, A. Logadottir, A. Carlsson, S. Dahl, C. H. Christensen, J. K. Nørskov, Science **2005**, *307*, 555–558.
[12] N. Furuya, H. J. Yoshiba, *Electroanal. Chem.* **1990**, *291*, 269–272.
[13] a) S.-J. Li, D. Bao, M.-M. Shi, B.-R. Wulan, J.-M. Yan, Q. Jiang, *Adv. Mater*. **2017**, *33*, 1700001; b) S. Mukherjee, D. A. Cullen, S. Karakalos, K. Liu, H. Zhang, S. Zhao, H. Xu, K. L. More, G. Wang, G. Wu, *Nano Energy*, **2018**, *48*, 217-226.
[14] M. A. Shipman, M. D. Symes, *Catal. Today* **2017**, *286*, 57–68.
[15] V. Kyriakou, I. Garagounis, E. Vasileiou, A. Vourros, M. Stoukides, *Catal. Today* **2017**, *286*, 2–13.

Accepted Manuscript

This article is protected by copyright. All rights reserved.

[16] G.-F. Chen, X.Cao, S. Wu, X. Zeng, L.-X. Ding, M. Zhu, H. Wang, J. *Am. Chem. Soc.* **2017**, *139*, 9771–9774.
[17] J. Zhao, Z. Chen, *J. Am. Chem. Soc.* **2017**, *139*, 12480–12487.
[18] S. Licht, B. Cui, B. Wang, F.-F. Li, J. Lau, S. Liu, *Science* **2014**, *345*, 637–640.
[19] G. Marnellos, M. Stoukides, *Science* **1998**, *282*, 98–100.
[20] S. Soll, M. Antonietti, J. Yuan, *ACS Macro Lett.* **2012**, *1*, 84–87.
[21] Y. Ding, X. Sun, L. Zhang, S. Mao, Z. Xie, Z.-W. Liu, D. S. Su, *Angew. Chem. Int. Ed.* **2015**, *54*, 231 –235
[22] H. Wang, J. Jia, Q. Wang, D. Li, S. Min, C. Qiana, L. Wang, C. Ma, T. Wu, J. Yuan, M. Antonietti, G. A. Ozin, *Angew. Chem. Int. Ed.* **2017**, *56*, 7847–7852.
[23] W. Ouyang, D. Zeng, X. Yu, F. Xie, W. Zhang, J. Chen, J. Yan, F. Xie, L. Wang, H. Meng, D. Yuan, *Int. J. Hydrogen. Energy*. **2014**, *39*, 15996.
[24] D. F. Bolt, Colorimetric Determination of Nonmetals, Wiley, 1978, Vol. 2.
[25] M. Schrinner, M. Ballauff, Y. Talmon, Y. Kauffmann, J. Thun, M. Möller, J. Breu, *Science* **2009**, *323*, 617–620.
[26] D. Bao, Q. Zhang, F.-L. Meng, H.-X. Zhong, M.-M. Shi, Y. Zhang, J-M. Yan, Q. Jiang, X.-B. Zhang, *Adv. Mater.* **2017**, 29, 1604799.
[27] R. J. White, R. Luque, V. L. Budarin, J. H. Clark, D. J. Macquarrie, *Chem. Soc. Rev.* **2009**, *38*, 481–494.
[28] C. Guo, J. Ran, A. Vasileffa, S.-Z. Qiao, *Energy Environ. Sci.* **2018**,*11*, 45-56.
[29] X.-H. Li, M. Antonietti, *Chem. Soc. Rev.* **2013**, *42*, 6593–6604.

WILEY-VCH
Accepted Manuscript

This article is protected by copyright. All rights reserved.

10.1002/anie.201805514

WILEY-VCH

Entry for the Table of Contents (Please choose one layout)

Layout 1:

COMMUNICATION

Nitrogen-doped carbon-based membrane nano(porous) electrocatalyst: A versatile and straightforward method was introduced to fabricate N-doped hierarchical porous carbon-based membrane, which can be directly utilized as highly active, selective and stable diffusion electrode for nitrogen fixation under ambient conditions.

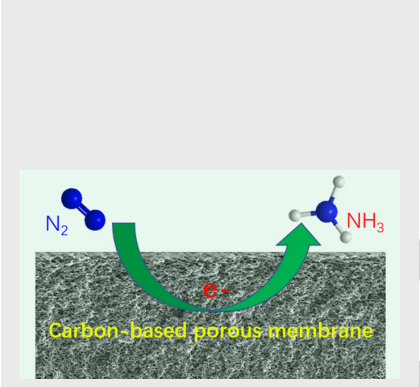

Hong Wang‡, Lu Wang‡, Qiang Wang, Shuyang Ye, Wei Sun, Yue Shao, Zhiping Jiang, Qiao Qiao, Yimei Zhu, Pengfei Song, Debao Li, Le He, Xiaohong Zhang, Jiayin Yuan*, Tom Wu, Geoffrey A. Ozin**

Page No. – Page No.

Title: Ambient Electro-Synthesis of Ammonia - Electrode Porosity and Composition Engineering

WILEY-VCH
Accepted Manuscript

This article is protected by copyright. All rights reserved.